Engineering of a complex bone tissue model with endothelialised channels and capillary-like networks

European Cells and Materials Vol. 35 2018 (pages 335-349) DOI: 10.22203/eCM.v035a23 ISSN 1473-2262

ENGINEERING OF A COMPLEX BONE TISSUE MODEL WITH ENDOTHELIALISED CHANNELS AND CAPILLARY-LIKE NETWORKS

B.J. Klotz[1,2], K.S. Lim[3], Y.X. Chang[1,2], B.G. Soliman[1,2,3], I. Pennings[1,2], F.P.W. Melchels[4], T.B.F. Woodfield[3], A.J.W.P. Rosenberg[1], J. Malda[2,5,6] and D. Gawlitta[1,2,*]

[1] Department of Oral and Maxillofacial Surgery and Special Dental Care, University Medical Centre Utrecht, Utrecht University, Utrecht, the Netherlands
[2] Regenerative Medicine Centre Utrecht, Utrecht, the Netherlands
[3] Department of Orthopaedic Surgery and Centre for Bioengineering and Nanomedicine, University of Otago, Christchurch, New Zealand
[4] Institute of Biological Chemistry, Biophysics and Bioengineering, School of Engineering and Physical Sciences, Heriot-Watt University, Edinburgh, UK
[5] Department of Orthopaedics, University Medical Centre Utrecht, Utrecht University, Utrecht, the Netherlands
[6] Department of Equine Sciences, Faculty of Veterinary Medicine, Utrecht University, Utrecht, the Netherlands

Abstract

In engineering of tissue analogues, upscaling to clinically-relevant sized constructs remains a significant challenge. The successful integration of a vascular network throughout the engineered tissue is anticipated to overcome the lack of nutrient and oxygen supply to residing cells. This work aimed at developing a multiscale bone-tissue-specific vascularisation strategy.

Engineering pre-vascularised bone leads to biological and fabrication dilemmas. To fabricate channels endowed with an endothelium and suitable for osteogenesis, rather stiff materials are preferable, while capillarisation requires soft matrices. To overcome this challenge, gelatine-methacryloyl hydrogels were tailored by changing the degree of functionalisation to allow for cell spreading within the hydrogel, while still enabling endothelialisation on the hydrogel surface.

An additional challenge was the combination of the multiple required cell-types within one biomaterial, sharing the same culture medium. Consequently, a new medium composition was investigated that simultaneously allowed for endothelialisation, capillarisation and osteogenesis. Integrated multipotent mesenchymal stromal cells, which give rise to pericyte-like and osteogenic cells, and endothelial-colony-forming cells (ECFCs) which form capillaries and endothelium, were used.

Based on the aforementioned optimisation, a construct of 8 × 8 × 3 mm, with a central channel of 600 μm in diameter, was engineered. In this construct, ECFCs covered the channel with endothelium and osteogenic cells resided in the hydrogel, adjacent to self-assembled capillary-like networks. This study showed the promise of engineering complex tissue constructs by means of human primary cells, paving the way for scaling-up and finally overcoming the challenge of engineering vascularised tissues.

Keywords: Co-culture, endothelial-colony-forming cells, mesenchymal stromal cells, capillaries, endothelium, culture medium, osteogenesis, vasculogenesis, gelatine-methacryloyl, hydrogel.

***Address for correspondence**: Debby Gawlitta, UMC Utrecht, Heidelberglaan 100, PO Box 85500, 3508GA Utrecht, the Netherlands.
Telephone number: +31 887557751 Email: D.Gawlitta@umcutrecht.nl

Introduction

Engineering of large, clinically-relevant sized tissue analogues remains challenging due to the need for vascularisation. Oxygen and nutrients have to be delivered homogeneously throughout an engineered tissue due to their limited diffusion distance, typically 100-200 μm, and low solubility (Carmeliet and Jain, 2000). Consequently, an engineered multiscale vascular network has to place the residing cells

in the bulk material within a limited (diffusion) distance from the nearest perfused vessel (Langer and Vacanti, 1999; Rouwkema and Khademhosseini, 2016). Native bone tissue is characterised by a dense vascular system that regulates bone development, homeostasis and fracture healing (Kanczler and Oreffo, 2008; Lafage-Proust *et al.*, 2015). In addition to delivering oxygen and nutrients, blood flow through the vasculature also transports cells and growth factors to bone defect sites (Lafage-Proust *et al.*, 2015). In vascularised tissues, the vascular network consists of macrovessels branching into a dense bed of capillaries (microvessels). *In vitro* pre-vascularisation strategies, compared to intraoperative preparation of scaffolds, integrate faster with the host vasculature (Levenberg *et al.*, 2005) and prevent necrosis in the central core of the construct (Butt *et al.*, 2007). In principle, pre-vascularisation approaches will allow immediate blood supply throughout the engineered tissue upon its implantation through anastomosis to the host's blood circulation (Rouwkema and Khademhosseini, 2016).

A major advancement in the field is achieved through the biofabrication of a thick bone-like tissue with macrovessel-like structures and subsequent culture under flow perfusion (Kolesky *et al.*, 2016). However, this approach is limited to the macroscale, due to the restricted spatio-temporal resolution in current biofabrication technologies (Lee *et al.*, 2014). Moreover, in order to bring all residing cells close to the perfusing media flow, the presence of dense capillary beds and angiogenic sprouts into the bulk material is essential. Endothelial cells have the ability for self-assembling into capillary-like beds when co-cultured with stabilising cells (Unger *et al.*, 2015). Thus, for the formation of a dense capillary bed, it is a logical approach to exploit the self-assembly capacity of endothelial cells for forming microvessels and connecting with the main channel by sprouting angiogenesis (Lee *et al.*, 2014). This current bottleneck in the field is addressed by seeding endothelial cells into the bulk material surrounding the engineered channels (Lee *et al.*, 2014) or by enabling sprouting from a macrochannel by providing a cell penetrable 3-dimensional (3D) matrix (Miller *et al.*, 2012).

The integration of the abovementioned approaches for pre-vascularisation strategies is the next step in engineering of complex bone tissue constructs. When multiscale pre-vascularised, osteogenically differentiated tissue constructs are engineered, multiple aspects are critical. To date, these have not yet been addressed in a holistic approach for osteogenically stimulated constructs that are pre-vascularised by both capillaries and endothelium-lined macrovessels. Engineering of prevascularised bone leads to biological and fabrication dilemmas. A capillary bed requires soft bulk matrices (Occhetta *et al.*, 2015), preferably lower than 4 kPa (Nichol *et al.*, 2010), while pronounced osteogenic differentiation of progenitor cells is supported by materials with compressive moduli of 15-30 kPa (Tan *et al.*, 2014; Wen *et al.*, 2014). Such stiff hydrogels, which are not cell permissive, are generally used for the fabrication process of macrovessel-like structures (Rouwkema and Khademhosseini, 2016). The resulting structurally stable channel structures are covered with endothelial monolayers (Hasan *et al.*, 2015; Kolesky *et al.*, 2016; Nichol *et al.*, 2010). However, these stiff biomaterial compositions would impair or even exclude cell migration and sprouting into the bulk material.

Besides satisfying the biological requirements of the biomaterial, it also remains challenging to select a suitable culture medium. Choosing one type of medium might affect the differentiation and performance of the combined cell types (Baldwin *et al.*, 2014; Rouwkema and Khademhosseini, 2016). For engineering pre-vascularised bone, the medium has to simultaneously allow for i) endothelialisation on the hydrogel surface, ii) capillarisation and sprouting, iii) osteogenesis. To the best of our knowledge, these three aspects have, so far, not been systematically assessed within one single construct. In tissue engineering, the final aim is to stimulate simultaneous differentiation of multiple cell types within one construct. Therefore, a synergistic combination of media and biomaterial composition that allow for all essential cell lineage commitments is highly desirable.

In this study, an integrated approach was presented – combining multiple human primary cells – to engineer a pre-vascularised and osteogenically differentiated tissue construct. A main central macrovessel-like structure covered by endothelium was engineered in a capillarised, early bone tissue. For this purpose, clinically-relevant cell types, being multipotent mesenchymal stromal cells (MSCs) and endothelial-colony-forming cells (ECFCs), were combined in gelatine-based hydrogels. Gelatine-methacryloyl (gelMA) was selected as the base material, due to its tailorable properties for various tissue engineering applications (Klotz *et al.*, 2016). Firstly, gelMA was tuned towards endothelialisation (in 2D) and MSC spreading in 3D bulk hydrogels. Secondly, an optimal culture medium was defined to support multiscale pre-vascularised and osteogenically committed gelMA constructs. Finally, a multiscale pre-vascularised network was fabricated, which was characterised by an endothelium-lined macrochannel, a capillary-like network and a formed bone-like tissue.

Materials and Methods

The outline of the present study is described in Fig. 1, where *N* refers to the number of experiments conducted with different donor combinations of the MSC-ECFC co-cultures and *n* to the number of replicates within an experiment. For the medium selection, 3 different MSC-ECFC donor

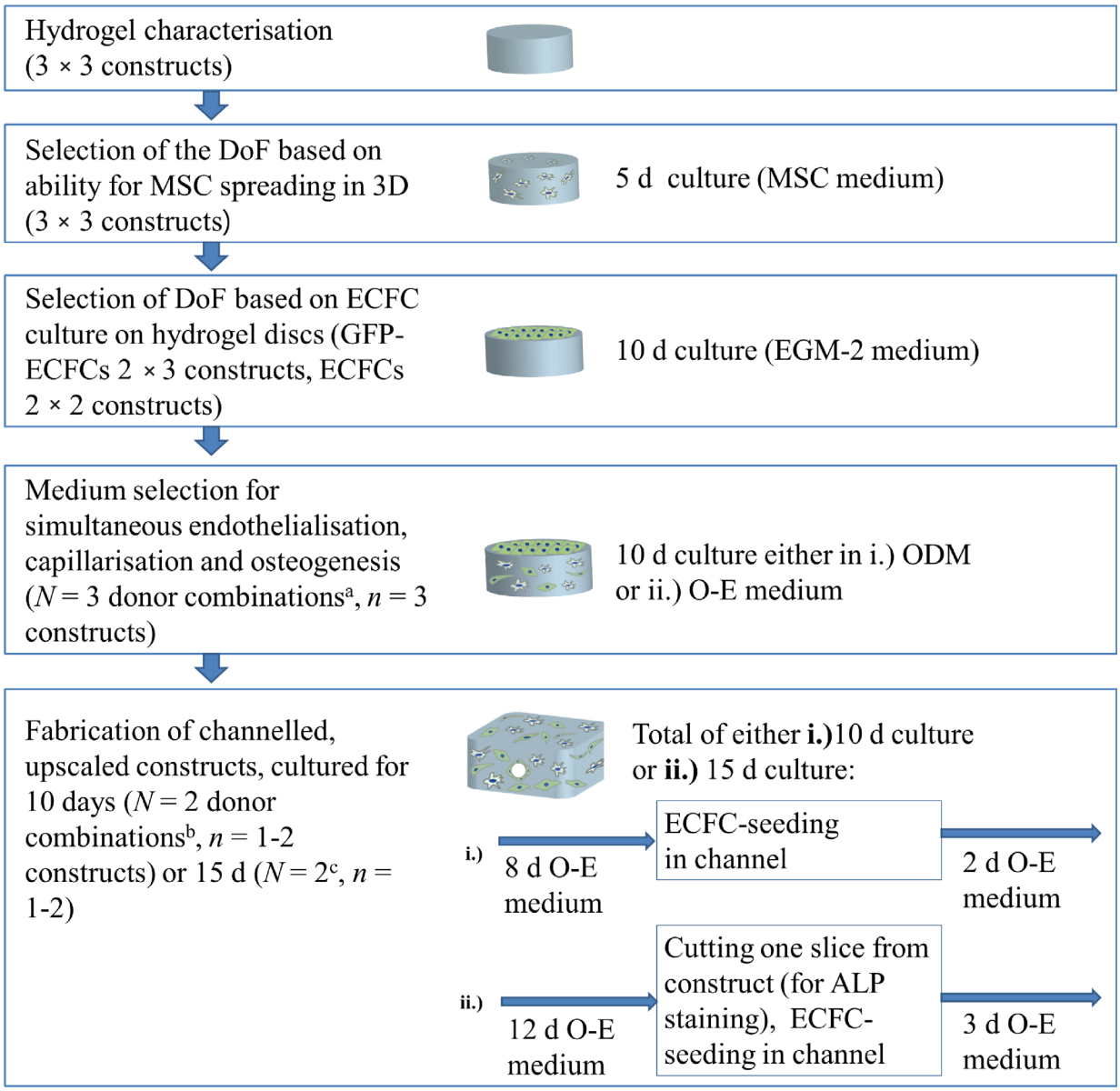

Fig. 1. Study outline and replicates. 3 independent experiments were performed for the hydrogel characterisation and MSC encapsulations. Cell seeding on hydrogel discs was performed twice with GFP-ECFCs and twice with non-labelled ECFCs. *N* refers to different experiments with varying MSC-ECFC combinations from different donors; *n* to the number of replicates within an experiment. Experiment a: MSC donor 1 + ECFC donor 1, MSC donor 1 + ECFC donor 2, MSC donor 2 + ECFC donor 2. Experiment b: MSC donor 2 + ECFC donor 1, MSC donor 2 + ECFC donor 2. Experiment c: MSC donor 2 + ECFC donor 1, MSC donor 3 + ECFC donor 1.

combinations were tested, with n = 3 replicates each. For the channelled constructs, N = 2 different MSC-ECFC donor combinations were tested, with n = 1-2 replicates and hydrogels cultured for 10 d. Furthermore, the same setup (N = 2, n = 1-2) was chosen for channelled constructs that were cultured up to 15 d. For the hydrogel characterisation, n = 3 independent experiments were performed, with n = 3 replicates (3 × 3 hydrogels). MSCs were encapsulated in hydrogels in n = 3 independent experiments, with n = 3 replicates (3 × 3 hydrogels). ECFC seeding on the hydrogel discs was performed twice for n = 2 independent experiments, with n = 3 replicates for GFP-labelled ECFCs, and twice with n = 2-3 replicates for non-labelled ECFCs.

Materials and mould preparations

Disc-shaped silicone moulds were prepared by punching 8 mm-diameter circles into silicone sheets of 1 mm in height (BioPlexus Corporation, Ventura, CA, USA). To make channelled hydrogel constructs, a custom-made mould (Med610, Stratasys, Eden Prairie, MN, USA) was designed with Autodesk Fusion 360 software version 2.0.3253, printed by Cetma (Brindisi, Italy) using an Objet30 3D printer (Stratasys). This mould (8 × 8 × 3 mm as inner

dimensions) served as the negative sample to prepare silicone moulds. Inlet and outlet ports in the mould were created by inserting a 0.6 mm-diameter needle into the printed construct. Sylgard 184 silicone elastomer kit (Dow Corning, Midland, MI, USA) was prepared according to the manufacturer's instructions and poured into the custom-designed mould. For hydrogel fabrication, silicone moulds (with needle insert) were placed onto a glass slide, where the gel solution was added and sealed from air by a second glass slide for subsequent UV crosslinking.

GelMA synthesis and characterisation

Gelatine was functionalised with methacryloyl groups to allow for free-radical-mediated photo-crosslinking of a thermally stable hydrogel. The physico-chemical and mechanical properties of the hydrogels can be further tailored by modifying the degree of functionalisation (*i.e.* number of methacryloyl groups). This is particularly important as the hydrogel microenvironment closely regulates the cell-matrix interaction, affecting cell attachment, spreading and proliferation. GelMA was prepared from type A porcine gelatine (MedellaPro, Gelita, Eberbach, Germany) that was reacted with methacrylic anhydride (Sigma-Aldrich), as described previously (Van den Bulcke *et al.*, 2000). In brief, gelatine was dissolved in phosphate buffered saline (PBS) by heating to 50 °C. Two batches of gelMA were prepared, one with a low- and one with a high-degree of functionalisation (DoF). 0.02 g and 0.6 g of methacrylic anhydride/g of gelatine, respectively, were added drop-wise to the solution and allowed to react for 1 h under constant stirring. Subsequently, unreacted methacrylic anhydride was removed from the reaction mixture by centrifugation. After the pH of the solution was set to 7.4, the gelMA solution was dialysed against distilled water using a cellulose membrane (14 kDa cut-off, Sigma-Aldrich) for 5 d at room temperature. The gelMA solution was sterile filtered, lyophilised and stored at − 20 °C until use. The DoFs of the two gelMA batches were determined by the ninhydrin assay, as described previously (Loessner *et al.*, 2016). The DoF is defined by the percentage of modified lysine residues (Van den Bulcke *et al.*, 2000) and was calculated to be 18.4 % (referred to as 20 %) and 78 % (referred to as 80 %) for the low and high DoF gelMA batches, respectively.

Hydrogel preparation

The gelMA precursor solution was crosslinked by UV-light using 0.1 % (w/v) Irgacure® 2959 (Ciba®, Ludwigshafen am Rhein, Germany). One day before use, GelMA solutions were heated to 70 °C for 15 min and the two batches were mixed in varying ratios to obtain final average DoFs between 30 % and 70 %. For hydrogel preparation, gelMA was dissolved at 60 °C and diluted with PBS to a final concentration of 5 %. Finally, the gelMA precursor solution with 0.1 % Irgacure® 2959 was pipetted into a mould and crosslinked in a UVP CL-1000L UV linker (UVP Cambridge, UK; 365 nm, 7 mW/cm²) for 15 min. Hydrogel constructs containing a channel were crosslinked from both sides for 4.5 min each, with a Superlite S-UV 201AV lamp (350-500 nm, Lumatec, Munich, Germany).

Mechanical analysis of hydrogel

GelMA hydrogels were prepared and incubated for 24 h in PBS at 37 °C (3 independent experiments with $n = 3$) and the compression modulus was determined by a Dynamic Mechanical Analyser (DMA, Q800 TA Instruments, New Castle, DE, USA) at room temperature. Compression was applied between – 20 %/min and −30 %/min and the Young's modulus was calculated from the slope of the linear region of the stress/strain curves in the 5-10 % strain range.

Mass loss and swelling studies

Mass loss and swelling studies were performed on GelMA hydrogels, as previously reported (Lim *et al.*, 2013). In short, the wet weight of the hydrogels was determined directly after crosslinking ($m_{initial,\ t0}$). Then, 3 out of 6 hydrogels per experimental group were frozen and lyophilised to obtain the dry weights of the hydrogels ($m_{dry,\ t0}$). The other 3 hydrogels were left in PBS at 37 °C for 24 h, frozen and lyophilised to obtain the dry weight ($m_{dry,t1}$). The hydrogel swelling ratio (q) and the sol fraction were calculated as described in the following equations (Lim *et al.*, 2012; Nilasaroya *et al.*, 2008):

$$Actual\ macromer\ fraction = \frac{m_{dry,\ t0}}{m_{initial,\ t0}}$$

$$q = \frac{m_{swollen}}{m_{dry,t1}}$$

$$m_{initial,dry} = m_{initial,t0}\ x\ actual\ macromer\ fraction$$

$$Sol\ fraction = \frac{m_{initial,dry} - m_{dry}}{m_{initial,dry}}\ x\ 100\ \%$$

Cell culture media

MSC expansion medium was composed of alpha modification minimum essential medium (α-MEM; Gibco), 10 % heat-inactivated foetal bovine serum (FBS; Lonza), 100 U/mL penicillin, 10 mg/mL streptomycin (Gibco), 0.2 mM L-ascorbic acid-2-phosphate (ASAP; Sigma-Aldrich) and 1 ng/mL fibroblast growth factor-2 (FGF-2; 233-FB, R&D Systems). Endothelial growth medium-2 (EGM-2) was composed of endothelial basal medium-2 (EBM; Lonza), 10 % FBS, 100 U/mL penicillin, 10 mg/mL streptomycin and EGM-2 SingleQuot (Lonza). Osteogenic differentiation medium (ODM) was composed of α-MEM, 10 % FBS, 100 U/mL penicillin, 10 mg/mL streptomycin, 10 mM β-glycerophosphate (Sigma-Aldrich) and 10 nm dexamethasone (Sigma-Aldrich). For the ODM-EGM combination medium (O-E), the osteogenic components β-glycerophosphate and dexamethasone were 2× concentrated and subsequently 1 : 1 diluted with EGM-2.

MSC isolation and culture

Bone marrow aspirates were obtained from the iliac crest of 3 donor patients after informed consent was given and with approval of the local ethics committee (TCBio-08-001-K University Medical Centre Utrecht, the Netherlands). The white mononuclear cell (MNC) fraction was collected after performing a density gradient centrifugation on Ficoll-Paque PLUS (1.077 g/mL; GE Healthcare). Obtained cells were cultured in MSC expansion medium at 37 °C/5.0 % CO_2 and tested for differentiation potential into osteo-, adipo- and chondrogenic lineages. Obtained MSCs were analysed by fluorescence-activated cell sorting (FACS) and were negative for the haematopoietic markers CD14 [RPA-M1, fluorescein isothiocyanate (FITC)-conjugated, Abcam], CD34 [4H11, alkaline phosphatase (AP)-conjugated, Abcam], CD45 [MEM-28, phycoerythrin (PE)-conjugated, Abcam] and CD79a (HM47, PE-conjugated, Abcam) and positive for the established MSCs markers CD90 (5E10, FITC-conjugated, Abcam), CD105 (MEM-226, AP-conjugated, Abcam) and CD73 (AD2, PE-conjugated, Abcam). For all the experiments, MSCs up to passage 4 were used.

ECFC isolation and culture

Human umbilical cord blood from 2 donors was obtained after approval by the local ethics committee (METC 01-230/K, University Medical Centre Utrecht, the Netherlands) and following patient informed consent after caesarean section. The blood was diluted at least 1 : 1 with PBS 2 mM EDTA and the MNC were isolated by density gradient centrifugation on Ficoll-Paque PLUS. Obtained cells were plated on rat tail collagen I (Corning)-coated plates at a seeding density of 10-20 × 10^6 cells/cm^2 and cultured in EGM-2. The culture medium was refreshed daily during the first 7 d after cell isolation and afterwards every 3-4 d. After 14-21 d, colonies with cobblestone morphology were picked and replated for expansion. Obtained ECFCs were analysed by FACS and resulted positive for CD105 and CD31 (TLD-3A12, FITC-conjugated, Abcam), partially positive for CD34 and CD309 (VEGFR/KDR, PE-conjugated, MACS, Miltenyi Biotech) and negative for CD45, CD14 and CD133 (AC133-VioBright, FITC-conjugated, Miltenyi Biotech). ECFCs were used up to passage 10 for all the experiments.

ECFC transduction with GFP

ECFCs in passage 5 were seeded at a density of 4700 cells/cm^2 and transduced with a lentiviral green fluorescent protein (GFP) construct (in a pHAGE2 vector combined with a human EF-1α promotor) in FBS-free medium the following day. After 1 d, fresh EGM-2 was added to the cells. Selection of ECFCs that were successfully transduced with the GFP-construct occurred by addition of 3 µg/mL puromycin (Sigma-Aldrich) for 10 d. During selection, GFP-ECFCs were expanded for 2 passages to create a batch of fluorescently-labelled cells.

Co-cultures in gelMA and discs covered with ECFCs

ECFCs and MSCs were co-cultured in 5 % gelMA hydrogels and, additionally, ECFCs were seeded on top of the hydrogel discs. Cell-encapsulation occurred in gelMA mixtures of 30 and 50 % DoF, as described above. For these hydrogels, PBS was replaced with the respective culture medium to encapsulate 1.25 × 10^6/mL ECFCs and 5 × 10^6/mL MSCs. Following hydrogel crosslinking, ECFC suspensions (6.6 × 10^5 cells/mL) were seeded on top of the disc and left to adhere for 30 min before medium was added. Constructs containing only a (GFP-)ECFC monolayer were cultured in EGM-2, whereas constructs containing a MSC/ECFC co-culture in the hydrogel and ECFCs on top of the disc were cultured in ODM or O-E. After 10 d of culture, gels were fixed and cut in half for vasculogenic and osteogenic stainings ($N = 3$, $n = 2$-3).

Preparation of MSC-ECFC containing channelled constructs

MSCs and ECFCs were encapsulated at 5 × 10^6 and 1.25 × 10^6 cells/mL, respectively, in 50 % DoF, 5% w/v gelMA constructs containing a channel that was seeded with ECFCs as follows. The cell-prepolymer-mixture was injected and cross-linked in silicone moulds with a 0.6 mm-diameter retractable needle in the centre to create the channel in the bulk hydrogel. The gels were cultured in O-E for 8 d before ECFCs, at a concentration of 50 × 10^6 cells/mL, were seeded into the channel. The cells were allowed to adhere for 15 min before the construct was flipped of 180° and incubated for another 15 min. Next, O-E was added for another 2 d. Alternatively, the gels were cultured for 12 d and a slice was cut from the construct for alkaline phosphatase (ALP) staining. In these gels, ECFCs were seeded at a concentration of 50 × 10^6 cells/mL on day 12 and the construct was further cultured up to day 15. The constructs were cultured for either 10 or 15 d in O-E, fixed and cut into sections for further analysis.

F-actin staining

MSCs were encapsulated at a concentration of 5 × 10^6 cells/mL in 30, 50 and 80 % DoF at 5 % w/v gelMA hydrogels (3 independent experiments with n = 3 hydrogel discs). After 5 d, the gels were fixed and stained whole mount with 0.2 µm tetramethylrhodamine B isothiocyanate (TRITC)-phalloidin (Sigma-Aldrich) after permeabilisation with PBS-Triton-X and a blocking step in 5% bovine serum albumin (BSA) in PBS. The central plane in the hydrogels were imaged using a confocal microscope (SP8x Leica, DMi8) to assess cell morphology in 3D.

Histology and immunostaining

After 10 or 15 d of culture, samples were fixed and stained for ALP activity using Fuchsin + Substrate-Chromogen System (K0624, Dako). For immunostainings, the samples were permeabilised with 0.2 % Triton-X in PBS for 30 min and blocked

in BSA/PBS for 30 min. The formation of stabilised capillary-like structures was assessed by CD31 staining (5.1 µg/mL; M0823, Dako), secondary sheep anti-mouse biotinylated antibody (1 : 200; RPN1001v1, GE Healthcare) and tertiary streptavidin Alexa Fluor 488 conjugate (5.0 µg/mL; S32354, Invitrogen). Mouse monoclonal Cy3-conjugated α-smooth muscle actin (αSMA) antibody (1 : 300; Clone 1A4, C6198, Sigma-Aldrich) was used to detect the stabilising cells of the capillary-like structures. Furthermore, anti-vascular endothelial cadherin antibody from rabbit (VE-cad, 1 : 250; D87F2, Cell Signalling Technology) was combined with Hilyte fluor 488 (2 µg/mL; AS-28176-05-H488, AnaSpec, Fremont, CA, USA) and murine anti-von Willebrand factor antibody (vWF, 8 µg/mL; ab194405, Abcam) with secondary Alexa Fluor 546 (A-11030, goat-anti-mouse, 2 µg/mL; ThermoFisher Scientific). 4, 6-diamidino-2-phenylindole (DAPI, 100 ng/mL; Sigma-Aldrich) was used to stain the cell nuclei. The constructs were imaged with an upright fluorescence microscope (BX51, Olympus) or confocal microscope (SP8x Leica, DMi8, Leica).

Immunohistochemistry

After fixation, hydrogels were dehydrated in graded ethanol series, cleared in xylene and embedded in paraffin. An osteonectin staining was performed on 5 µm-thick sections. In short, sections were deparaffinised and hydrated before endogenous peroxidase was blocked in 0.3 % H_2O_2. Antigen retrieval was performed in citrate buffer at 80 °C for 20 min. Subsequently, the primary antibody for osteonectin [4.2 µg/mL; AON-1 was deposited to the Developmental Studies Hybridoma Bank (DSHB) by J.D. Termine (Bolander *et al.*, 1989)] was incubated for 1 h before addition of a horseradish peroxidase-conjugated anti-mouse antibody (EnVision + System-HRP Labelled Polymer, K4000, Dako). Osteonectin was detected by conversion of 3,3'-diaminobenzidine solution (SK-4100, Vector, Burlingame, CA, USA) and nuclei were counterstained with haematoxylin (Merck). Isotype controls were performed using concentration-matched mouse IgG1 monoclonal antibody (ThermoFisher Scientific).

Image analysis

RGB fluorescence images of the whole hydrogel construct (one field of view per hydrogel, with a random selected plane) were obtained using an upright fluorescence microscope (BX51, Olympus). Images were merged, where contrast and intensity were set to be comparable across all images using

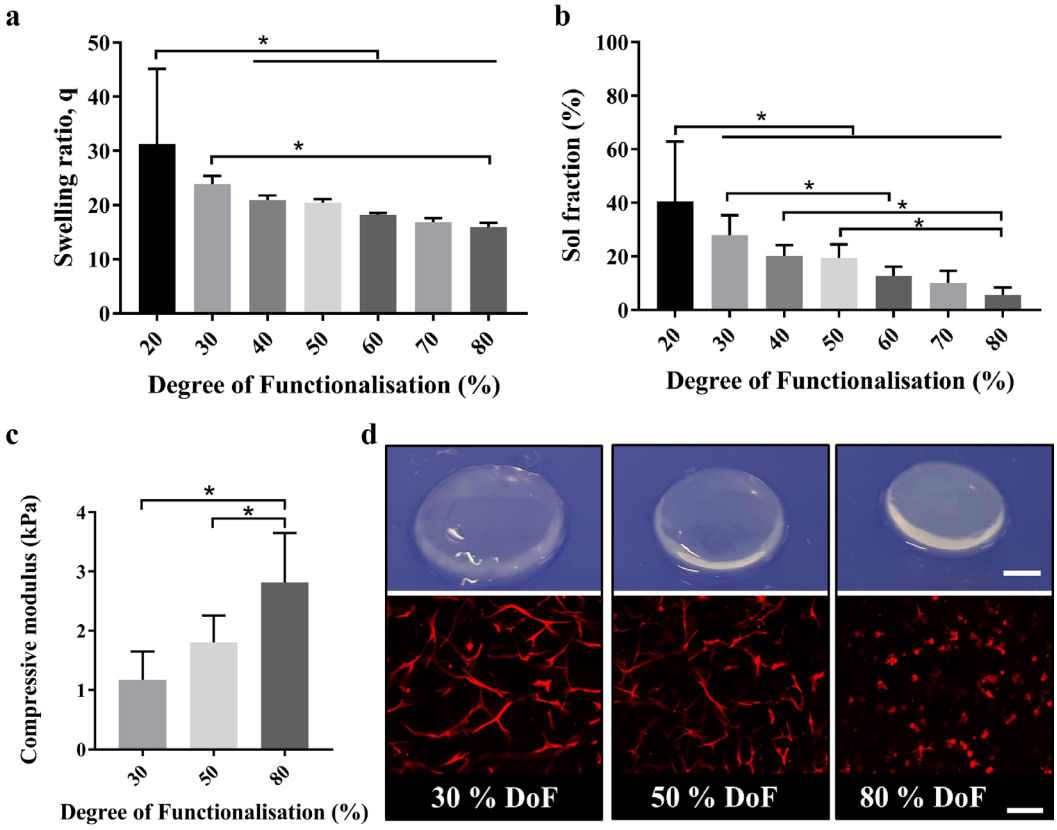

Fig. 2. GelMA hydrogel characterisation based on physico-mechanical and biological aspects. 5 % GelMA hydrogels, with average DoF ranging from 20 to 80 %, were characterised. (**a**) Swelling ratio and (**b**) sol fraction gradually decreased from 20 % DoF hydrogels to 80 % DoF. (**c**) Compressive moduli of gelMA hydrogels increased with increasing DoF. (**d**, upper row) A decrease in hydrogel swelling was macroscopically visible with increasing DoF; scale bar: 2 mm. (**d**, bottom row) MSC encapsulation in 30, 50 and 80 % DoF gelMA hydrogels resulted in cell spreading in 30 and 50 % DoF hydrogels, whereas MSCs stayed rounded in 80 % DoF gelMA hydrogels at day 5; TRITC-phalloidin; scale bar: 200 µm.

Adobe Photoshop CS6 and ImageJ 1.47v and 1.51a. Total and mean lengths of vessel-like structures were quantified by manual processing by AngioQuant software, as per previously published protocols (Niemisto *et al.*, 2005). Quantification of cell-based experiments was based on 3 experiments with different MSC-ECFC donor combinations (N = 3) and 2-3 gels (n = 2-3) per condition. In total, 9 field of views of 9 different hydrogels were quantified for the O-E condition and 8 hydrogels were imaged for the ODM condition.

Statistical analysis

Difference of the means between O-E and ODM cultures of the AngioQuant data was determined by Student's t-tests in GraphPad Prism 7.02. The significance of the differences in the mean compressive moduli, sol fractions and swelling ratios were detected by a one-way ANOVA and subsequent Tukey honest significant difference (HSD) *post-hoc* analysis using GraphPad Prism 7.02. $p < 0.05$ was considered significant.

Results

GelMA hydrogel optimisation by tuning the DoF

The DoF was optimised for 5 % gelMA hydrogels, in order to select a composition with suitable physico-mechanical and biological properties to engineer pre-vascularised bone constructs. While a high swelling ratio, indicated by water uptake of the hydrogel, provides cells with freedom to migrate (Ehrbar *et al.*, 2011), it is also associated with loss of material during the crosslinking process (sol fraction), which should be kept minimal (Nandi and Winter, 2005). Hydrogels with a DoF ranging from 20 % to 80 % gradually decreased in swelling ratio from 31.3 ± 13.4 to 16 ± 0.7 ($p < 0.0001$) (Fig. 2**a**). Also, the sol fraction decreased, with increasing DoF, from 40.5 ± 21.8 % to 5.5 ± 2.7 % ($p < 0.0001$) (Fig. 2**b**). The compressive modulus indicates the bulk stiffness of the hydrogel and is used to determine the range of mechanical properties that support cell spreading and migration in 3D (Ehrbar *et al.*, 2011). The compressive modulus slightly increased from 1.2 ± 0.5 kPa (30 % DoF hydrogel) to 1.8 ± 0.5 kPa ($p = 0.0966$) and 2.8 ± 0.8 kPa (30 *vs.* 80 $p < 0.0001$, 50 *vs.* 80 $p = 0.0052$) for 50 % and 80 % DoF hydrogels, respectively (Fig. 2**c**). Macroscopically, a difference in swelling behaviour was visible among 30 %, 50 % and 80 % DoF hydrogels (Fig. 2**d**, upper row). Biologically, a clearly varying cell response was observed among these three hydrogel compositions. After 5 d, MSCs spread in 30 and 50 % DoF hydrogels, which did not occur in 80 % DoF (Fig. 2**d**, bottom row). Since cell spreading is essential for the assembly of pre-vascular structures, 30 and 50 % DoF hydrogel compositions were selected for further studies.

Evaluation of endothelium formation

A further selection between 30 and 50 % DoF gelMA was made by evaluating the suitability for formation of endothelial monolayers on the hydrogel surface.

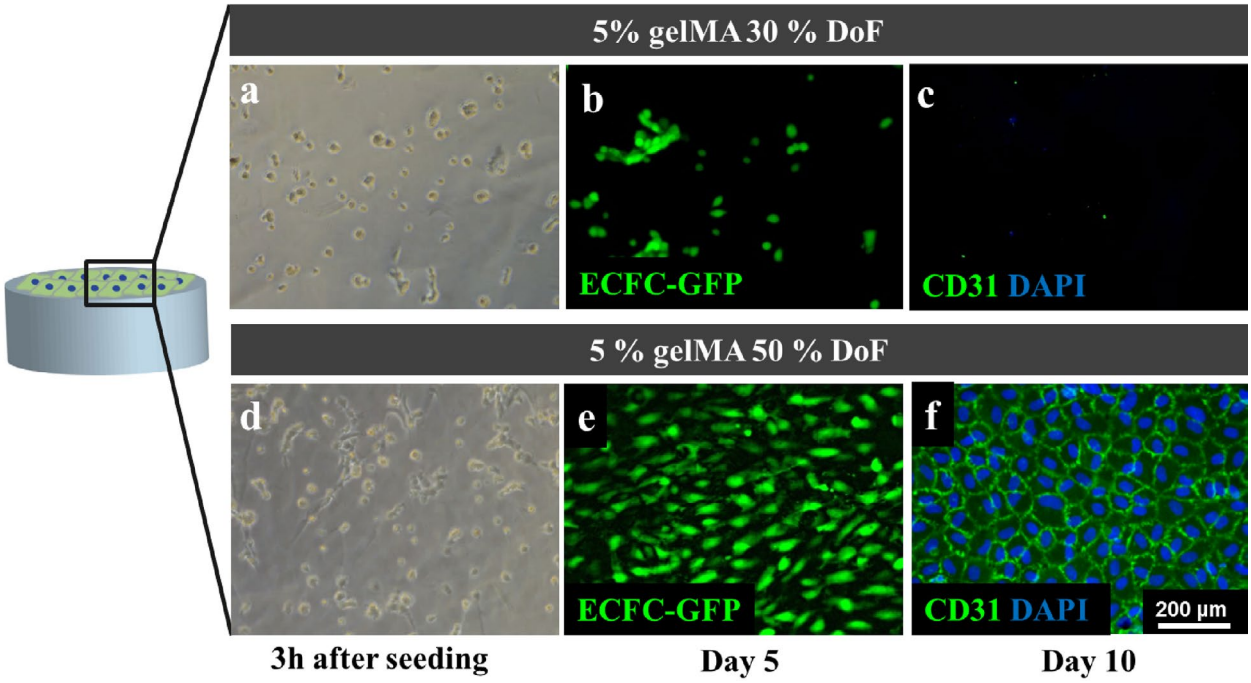

Fig. 3. Effect of gelMA DoF on ECFC monolayer formation on hydrogel discs cultured for up to 10 d. (**a**,**b**) GFP-labelled ECFCs attached to a 30 % DoF gelMA hydrogel surface 3 h after seeding and after 5 d, however, (**c**) after 10 d, cells were detached when cultured in EGM-2 (2 out of 4 experiments). (**d**-**f**) GFP-ECFCs were able to attach to 50 % DoF gelMA hydrogels and form an endothelial monolayer when cultured in EGM-2 (N = 2, n = 2-3).

ECFCs that were seeded on 30 % DoF hydrogels did not allow for reproducible monolayer formation since the cells detached over time in culture in 2 out of 4 experiments (Fig. 3**a**-**c**), whereas on 50 % DoF hydrogels, endothelial cells were able to robustly form confluent monolayers (Fig. 3**e**,**f**). Based on these results, 50 % DoF gelMA hydrogels were selected to create multi-scale pre-vascularised bone constructs.

Optimisation of culture medium for pre-vascularisation and osteogenesis

The culture medium composition was optimised for pre-vascularisation and osteogenic commitment of encapsulated cells in the bulk hydrogel. Also, the medium had to allow for ECFC monolayer formation on the hydrogel surface, given that any macrovessel or channel in the hydrogel would preferably be covered with endothelium. Whereas the biomaterial selection (Fig. 3) was based on constructs that were cultured in the preferred medium for ECFCs (EGM-2), the MSC-ECFC co-cultures were cultured in either ODM or O-E.

The constructs cultured in ODM resulted in impaired ECFC monolayer formation on the hydrogel surface (Fig. 4**a**), whereas in the O-E, ECFC-monolayers were obtained reproducibly (Fig. 4**d**). Pre-vascular network formation in the bulk hydrogel was more pronounced in O-E as compared to ODM (Fig. 4**b**,**e**). Also, the total length of vessel-like structures was significantly greater in O-E cultures when compared to ODM (p = 0.0168) (Fig. 4**g**,**h**). Addition of 50 % EGM-2 to the ODM resulted in an ALP activity comparable to constructs that were cultured in 100 % ODM (Fig. 4**c**,**f**).

Characterisation of endothelium, capillaries and pericyte-like cells

Along with the expression of CD31, indicating the formation of capillary-like structures, the phenotype of the endothelial cells was further investigated after culture for 10 d in O-E. VE-cadherin highlighted the presence of intercellular junctions between endothelial cells, both in the endothelium (Fig. 5**a**) and in the capillary-like structures inside the bulk hydrogel (Fig. 5**b**). The adhesive glycoprotein vWF, synthesised by endothelial cells, formed globular structures in the cytoplasm (Fig. 5**a**,**b**). Pericyte-like cells adjoining the endothelial structures were identified by positive staining for αSMA (Fig. 5**c**). Furthermore, the interface between the endothelium-covered hydrogel surface and the bulk hydrogel with capillary-like structures was investigated (Fig. 5**d**). Co-existence of stabilised capillaries in direct contact with an endothelial monolayer could show the feasibility that differentiated MSCs did not impede the formation of the endothelium. Three

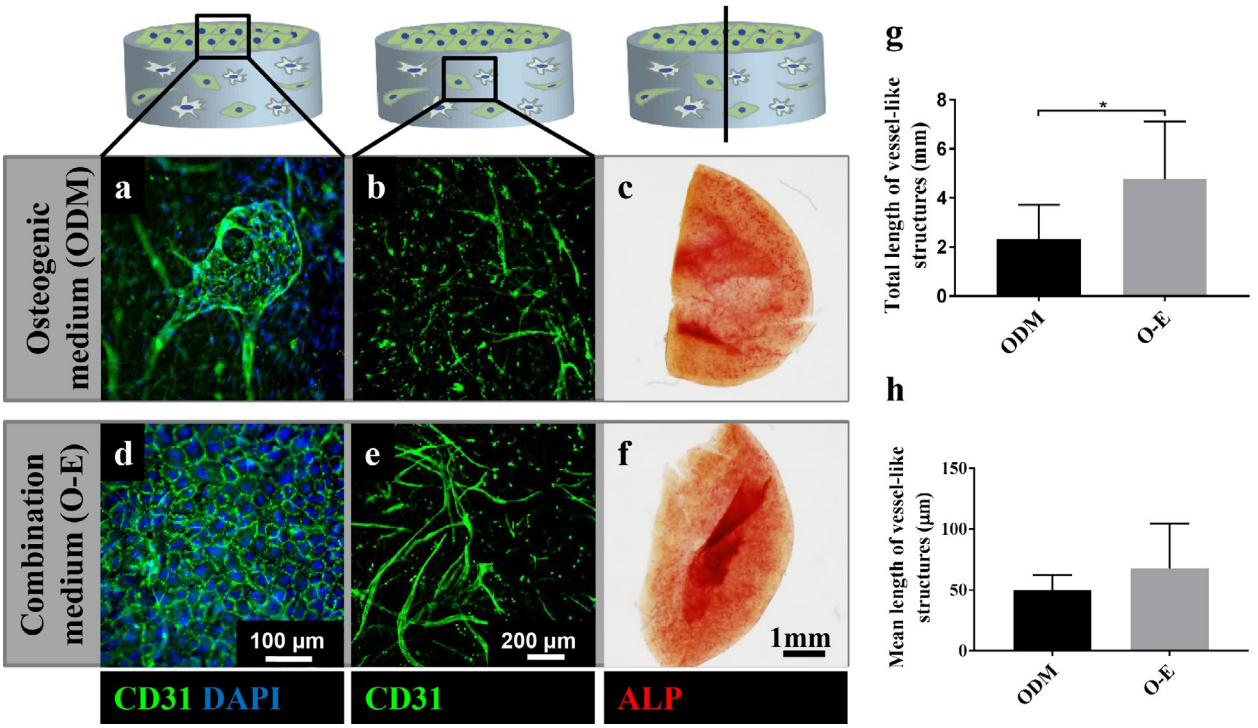

Fig. 4. Influence of media composition on ECFC monolayer formation on top of 5 % gelMA discs (50 % DoF) and on capillary-like structure assembly and osteogenic differentiation of ECFC-MSC co-cultures inside gelMA discs. (**a**) Endothelial monolayer formation was impaired in ODM, whereas in (**d**) O-E, endothelial monolayer patches were present after a culture time of 10 d. (**b**,**e**) Capillary-like structure formation in the bulk hydrogel was dependent on the culture medium. (**c**,**f**) ALP activity was comparable in both co-cultures. (**g**,**h**) Quantification of total and mean vessel-like structure length showed the beneficial effect of the combination medium over ODM (N = 3, n = 2-3).

cross-sections at the level of the endothelium (Fig. 5**e**), transition zone (Fig. 5**f**) and capillary-like structures in the hydrogel (Fig. 5**g**) were analysed. An endothelial monolayer had formed on the hydrogel surface, with capillary-like structures extending from here into the bulk hydrogel (Fig. 5**g**). At the same time, capillary-like structures and αSMA-positive cells were present inside the hydrogel.

Engineering a macrovessel-like structure in a bulk hydrogel of capillaries and osteogenic cells

Multiscale pre-vascularised and osteogenically differentiated gelMA-based constructs were prepared and cultured for 10 d (Fig. 6**a**-**d**) and 15 d (Fig. 6**e**-**j**). These constructs contained MSC-ECFC co-cultures in the bulk hydrogel and a confluent ECFC monolayer in the macrochannel (Fig. 6). The luminal side of the channel was prominently covered with endothelial cells, with characteristic cobblestone-like morphology (Fig. 6**d**,**f**). Furthermore, sections showed capillary-like structures inside the surrounding bulk hydrogel of the constructs cultured for 10 d (Fig. 6**b**) and 15 d (Fig. 6**e**). Sprouting angiogenesis was present from the channel surface into the bulk hydrogel as seen in a cross-sectional projection of the channel (Fig. 6**b**). Here, αSMA-expressing cells covered the luminal side of the channel, which was additionally covered with endothelial cells (Fig. 6**c**, originating from the stack shown in Fig. 6**b**). Early osteogenic differentiation of MSCs, as shown by ALP activity, was observed after 12 d (Fig. 6**g**). Furthermore, osteonectin was produced by the cells after 15 d of culture (Fig. 6**h**,**i**).

Discussion

Vascularisation, in combination with tissue specific maturation, is one of the main challenges in tissue engineering when proceeding towards clinically-relevant sized tissue constructs (Klotz *et al.*, 2016). An often-used strategy is to create vessel-like structures in the form of engineered endothelial-seeded channels to enable vascular supply throughout the construct (Kolesky *et al.*, 2016; Kolesky *et al.*, 2014). Furthermore, endothelial cells have the capacity to self-assemble into a capillary bed, which extends

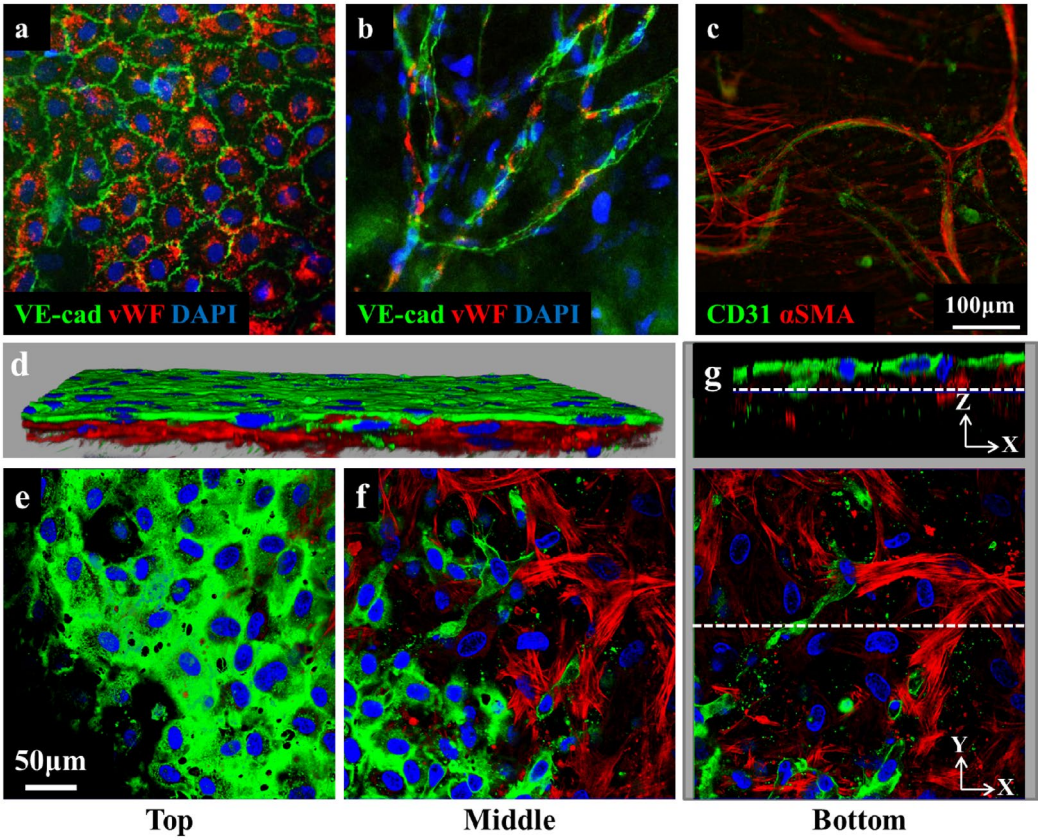

Fig. 5. Characterisation of endothelium, capillaries and pericyte-like cells in 5 % gelMA (50 % DoF) hydrogels cultured for 10 d in O-E. (**a**) Endothelial monolayers on the hydrogel surface show characteristic intercellular junctions enabled by VE-cadherin and vWF in the cytoplasm. (**b**) Capillary-like structures in the hydrogel expressed VE-cadherin and vWF. (**c**) Capillary-like CD31 structures adjoined with stabilising αSMA-positive pericyte-like cells. (**d**) Overview of interface between surface and hydrogel; CD31 in green, αSMA in red and nuclei in blue. (**e**) Endothelial monolayer forming an endothelium on the surface of gelMA hydrogel discs (X-Y axis). (**f**) Transition zone between endothelium and underlying capillary-structures and αSMA-expressing stabilising cells. (**g**) Cross-sections (Z-X and Y-X) showing capillary-like structures and stabilising cells inside the gelMA bulk hydrogel.

the vascular network through connections with the engineered channels (Lee *et al.*, 2014). This strategy of interconnected macrochannels and capillaries was advanced to the next stage by tailoring it specifically to bone tissue engineering based on clinically-relevant cell sources. In this work, it was demonstrated that multiple sub-cultured primary cell types could be supported within a single construct by means of tailored biomaterial physico-mechanical properties and cell-specific soluble cues in the medium. For the first time, a complex pre-vascularised bone model was realised that allowed for the formation of a multiscale vascular-like network within a developing bone-like matrix.

Fine-tuning of gelMA hydrogel characteristics

GelMA hydrogels can be adjusted for different applications by varying the gelatine source, polymer concentration, DoF or conversion of double bonds (*e.g.* through UV exposure time) (Klotz *et al.*, 2016; Nichol *et al.*, 2010; Van den Bulcke *et al.*, 2000). Even though osteogenesis predominantly occurs in stiff matrices with an elastic modulus of 11-30 kPa (Huebsch *et al.*, 2010; Tan *et al.*, 2014), the need for capillaries infiltrating the developing bone tissue requires the design of a soft gelMA matrix, preferably with an elastic modulus lower than 4 kPa (Nichol *et al.*, 2010). Furthermore, to enable the formation of an endothelium, the hydrogel composition has also to allow the ECFCs to develop a cobblestone-like phenotype on the hydrogel surface (Gimbrone *et al.*, 1974).

To obtain a hydrogel that was suitable for endothelialisation, vascularisation and osteogenesis, the physico-chemical and mechanical properties had to be precisely tailored and extensively characterised. It was possible to form 5 % gelMA hydrogels with a DoF as low as 20 %. However, the sol-gel characteristics of these hydrogels were not as reproducible as at higher DoFs, as shown by high standard deviations for sol fraction and mass swelling ratios. Therefore, 30 % DoF hydrogels with a compressive modulus of 1.2 ± 0.5 kPa were selected for further studies. While 5 % gelMA hydrogels (30 % DoF) performed best in terms of 3D MSC spreading, serving as an indicator of whether ECFCs could migrate and form capillary-like networks, this hydrogel composition is limited by its physico-mechanical characteristics. The pronounced swelling behaviour and the related structural instability excluded this composition for

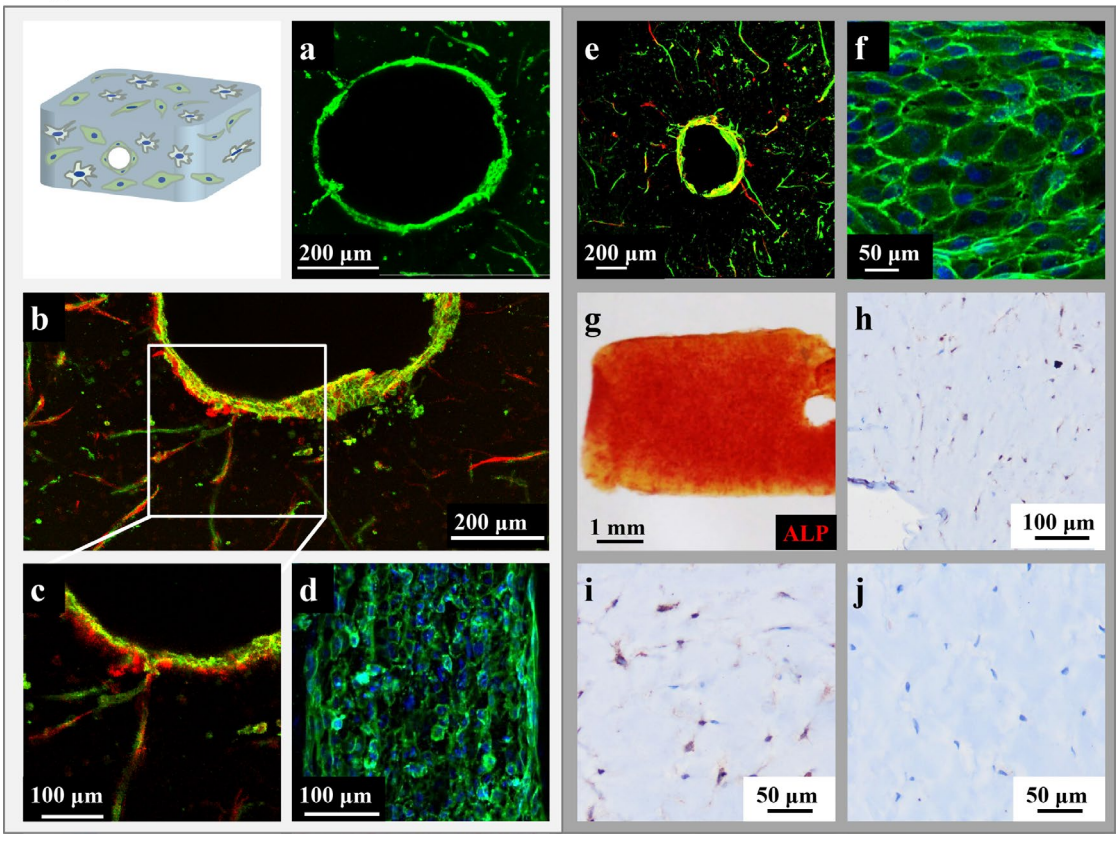

Fig. 6. Multiscale pre-vascularised and osteogenically differentiated gelMA constructs. Constructs prepared from 50 % DoF gelMA hydrogels containing ECFC-MSC co-cultures and an ECFC-seeded macrochannel were cultured in O-E for (**a**-**d**) 10 d or (**e**-**j**) 15 d. (**a**,**e**) Cross-section (projection) through the endothelialised channel, (**b**) projection of close-up of sprouts connecting with the channel-surface and (**c**) single image of stack in **b**. (**d**) Longitudinal section (projection) of endothelialised channel. (**f**) Projection of an endothelialised channel. (**g**) Slice of construct harvested after culture for 12 d for ALP staining. (**h**,**i**) Osteonectin staining of gelMA construct, cultured for 15 d and (**j**) isotype control. Staining in green for CD31, in red for αSMA and in blue for nuclei (at day 10 and day 15, each $N = 2$, $n = 1$-2).

the intended fabrication approaches. Furthermore, and in contrast to 50 % DoF gelMA hydrogels, 30 % DoF gelMA did not allow for reproducible ECFC attachment onto the surface of the hydrogel disc. This behaviour might be attributed to the considerable swelling of this hydrogel composition, leading to a reduced actual polymer concentration, which does not provide enough cell attachment sites. Pore sizes for gelMA hydrogels increase with decreasing DoF (Chen *et al.*, 2012) and might lead to a pore size that cannot be bridged anymore by residing cells on the hydrogel surface. Furthermore, hydrogels degrade faster with decreasing DoF (Chen *et al.*, 2012; Koshy *et al.*, 2014; Nguyen *et al.*, 2015), favouring, from a structural point of view, the higher DoF of 50 % over 30 %. In addition, no significant difference in compressive modulus was measured when the DoF of 5 % gelMA hydrogels was decreased from 50 % to 30 % ($p = 0.0966$). Therefore, 5 % gelMA at 50 % DoF represented a balance between biological and physico-mechanical requirements, as confirmed by an earlier study using this composition to engineer vascularised hydrogels (Chen *et al.*, 2012). These results highlighted an optimised fabrication window for soft gelMA hydrogels down to 5 % gelMA and 50 % DoF using Irgacure® 2959 as photo-initiator. This composition fulfilled the needed requirements of being relatively form-stable, allowing for endothelialisation on the hydrogel surface and enabling cell spreading within the hydrogel, which is needed for capillarisation.

Optimisation of culture medium composition for pre-vascularised bone

Medium selection is a critical element in culturing of complex tissue constructs containing multiple cell types. Typically, cell culture media are tailored for each individual cell type and vary, for instance, in composition of supplements, salts and vitamins (Baldwin *et al.*, 2014). While many approaches are reported to test the best medium conditions in mesenchymal and endothelial co-cultures for pre-vascularised bone tissue (Baldwin *et al.*, 2014; Bersini *et al.*, 2016; Jin *et al.*, 2015; Kolbe *et al.*, 2011; Ma *et al.*, 2011; Unger *et al.*, 2015), the effect of the same culture medium on endothelialisation of 2D hydrogel surfaces has not yet been reported. ODM performs best in 3D co-cultures of MSCs and endothelial cells for osteogenesis and vasculogenesis/angiogenesis (Gawlitta *et al.*, 2012; Ma *et al.*, 2011). However, in the present study, ODM did not allow for sufficient endothelialisation on gelMA hydrogel surfaces. A possible explanation could lie in the spatial separation of ECFCs and MSCs. Whereas ECFCs inside the hydrogels are stimulated by paracrine signalling from the co-embedded MSCs (Gruber *et al.*, 2005; Hung *et al.*, 2007), on the hydrogel surface (and in the presence of ODM without EGM-specific growth factors) ECFCs may have insufficient stimulating factors to survive and proliferate. Consequently, an alternative culture medium was investigated to allow for endothelialisation under osteogenic stimulation. Besides ODM, a variety of mixtures of ODM and EGM are reported to have been tested on co-cultures (Baldwin *et al.*, 2014; Jin *et al.*, 2015). Since these mixtures lead to a dilution of the osteogenic supplements, in the current study, the effects of a combination medium that contained double concentrated ODM (for β-glycerophosphate and dexamethasone) and standard EGM-2 in a 1 : 1 ratio (resulting in standard ODM component concentrations in the final O-E) were investigated. This medium allowed for more robust endothelialisation on co-culture-seeded gelMA hydrogel surfaces than ODM alone. VE-cadherin staining highlighted the formation of intercellular junctions between ECFCs and vWF was produced after 10 d. vWF was present in the cytoplasm of ECFCs and appeared as punctate globules, which is a characteristic of endothelial cells (Zheng *et al.*, 2015). These observations demonstrated the maintenance of the endothelial monolayer phenotype during the 10 d of culture in O-E. Furthermore, differentiation of pericyte-like cells under these culture conditions was confirmed by the presence of stabilising cells of endothelial structures, which were positive for αSMA. MSCs in co-culture with endothelial cells stabilise capillaries as pericyte-like cells (Au *et al.*, 2008). While the stabilising nature of these cells can be shown using different stainings, the identification of these cells as pericytes remains controversial, since there is a lack of distinct markers (de Souza *et al.*, 2016).

Capillary-like structures were present in constructs cultured in ODM; however, vasculogenesis was enhanced in the combination medium. At the same time, early osteogenesis was confirmed in constructs cultured in ODM and O-E. Previously, 1 : 1 diluted combination media have failed to induce mineralisation of cell-laden constructs (Gawlitta *et al.*, 2012; Ma *et al.*, 2011). Impaired mineralisation could be associated with the dilution of osteogenic supplements and might be a sign that a certain threshold of osteogenic supplements is required (Ma *et al.*, 2011). Lee *et al.* (2013) investigate a medium based on full EGM-2 supplemented with standard concentrations of osteogenic additives. However, this medium fails to induce mineralisation when compared to conventional ODM. Consequently, it is hypothesised that ingredients such as FGF-2, which is present in full EGM-2, might counteract robust osteogenic differentiation (Blache *et al.*, 2016). EGM-2 contains a complex mixture of different growth factors to support proliferation and maintenance of the endothelial phenotype and might, therefore, influence osteogenesis when used undiluted.

In light of clinical applications, it will be necessary not only to replace the serum, but also to limit the use of growth factors (GFs) to a minimum. Standard EGM-2 contains a cocktail of GFs and might be further fine-tuned and reduced to a few essential vasculogenic supplements in a combination medium. To do so, high-throughput screening platforms, such as presented by Bersini *et al.* (2016), will prove very

valuable. Besides screening for 3D co-culture aspects, it will be inevitable to screen the same media as well for 2D endothelialised hydrogel surfaces.

Engineering a macrovessel-like structure in pre-vascularised, osteogenically differentiated hydrogels

To proceed to a multiscale pre-vascularised, osteogenically differentiated construct model, an ECFC-seeded channel was engineered. It was feasible to obtain endothelialised channel surfaces, as well as newly sprouted vessel-like structures into these soft, complex cellular hydrogel constructs. This result differed significantly from previous works where endothelialised channels are created either under purely vasculogenic conditions, with non-clinically-relevant fibroblast or pericyte cell lines (Kolesky *et al.*, 2016; Lee *et al.*, 2014; Miller *et al.*, 2012), or in stiff osteogenesis-supporting matrices that do not allow for vasculogenic sprouting in the bulk hydrogel (Kolesky *et al.*, 2016).

Besides the characteristic endothelium with cobblestone morphology, capillary-like structures were also observed on the luminal side of the channel surface (not shown). These endothelial cords were only present in constructs containing MSC-ECFC co-cultures and not in ECFC-only (on the surface) constructs (not shown). ECFCs were seeded after an initial pre-differentiation phase, allowing for osteogenic differentiation and vasculogenesis to occur throughout the bulk of the hydrogel. A delay of 8 d appeared most favourable to establish an endothelium in the channel. After a pre-differentiation phase of 12 d, the channels were locally blocked by the cells and required clearing for ECFCs to be seeded. When ECFCs were seeded from the beginning in the channel of the cell-laden constructs, capillary-like monolayers were exclusively detected (data not shown), in agreement with previous studies (Bertassoni *et al.*, 2014; Byambaa *et al.*, 2017; Kazemzadeh-Narbat *et al.*, 2017; Zhu *et al.*, 2017). Surprisingly, this rather undesirable phenomenon of endothelial cords at the gel surface does not attract attention in the literature, while it seems to be an important challenge in the field. A simplified model disc was used to test whether MSC-derived cells would interfere with endothelium formation. On these discs, endothelium co-existed next to capillary-like structures, which were stabilised by αSMA-positive cells. Consequently, cell-cell contact with MSC-derived cells did not lead to disturbance of this monolayer.

The upscaled constructs exhibited an ALP activity level after 12 d that was comparable to hydrogel discs after 10 d. With a comparable hydrogel composition of 5 % gelMA (57 % DoF), the embedded rat MSCs show increased ALP activity on day 14 (Celikkin *et al.*, 2018). In the long term, this gelMA composition outperforms 10 % gelMA hydrogels in terms of the extend of calcium deposition and homogeneous distribution throughout the scaffold after 21 d (Celikkin *et al.*, 2018). In the present study, the presence of osteonectin was observed in constructs cultured for 15 d, highlighting ongoing osteogenesis along with vasculogenesis. The osteonectin staining was rather weak, which could be explained by the early time point for investigating osteogenesis. Matrix mineralisation and elevated osteogenic protein levels are normally assessed after culture periods of more than 3 weeks (Gotman *et al.*, 2013). The aim of the current study was to find a balance between two complex tissue developmental processes, vascularisation and osteogenesis, which required a pre-differentiation phase of the channelled constructs before ECFC-seeding into the channel. While the differentiation phase is relatively short to successfully prime *in vitro* osteogenesis, the optimal pre-differentiation period before implantation of such constructs remains to be investigated. Interestingly, prolonged *in vitro* cultures of MSCs in osteogenic media has a negative effect on the bone regeneration capacity in an orthotopic site (Castano-Izquierdo *et al.*, 2007). Moreover, long-term culture of these pre-vascularised constructs under static condition without perfusion is impractical, as the newly formed vessels will regress and rupture in the absence of a fluid flow (Urbaczek *et al.*, 2017). Hence, future studies will focus on a more thorough assessment of the differentiated osteogenic phenotype and mineralisation, in combination with perfusion, for successful clinical translation of the pre-vascularised bone model reported here.

The combination of multiple human primary cells in one tissue-engineered construct resulted in a viable approach. To further proceed towards preclinical applications, next steps will lie in upscaling and also mechanically stabilising these soft constructs. For instance, a 3D bioassembly approach can be employed to anatomically populate these soft pre-vascularised gelMA tissue modules into 3D plotted thermoplastic constructs (Mekhileri *et al.*, 2018). Mechanical reinforcement can also be achieved by combining these soft gelMA hydrogels with thermoplastic materials (Schuurman *et al.*, 2011; Boere *et al.*, 2014; Visser *et al.*, 2015; Mekhileri *et al.*, 2018), to withstand the mechanical forces in a bone defect site. To further promote the construct's *in vitro* maturation prior to implantation, flow perfusion might be needed to functionally interconnect the lumina of capillaries and the central channel into an intricate network. Ultimately, the engineered macrovessel-like structures need to be anastomosed to the circulation of a host animal to aid a fast vascularisation of the construct for tissue integration.

The rationale of this study was to advance the strategy of fabricating multi-scale vascularised networks in bone tissue engineering. Subcultured primary cell types were employed to mimic the biological intricacy of this tissue engineering approach, which enabled the investigation of its feasibility and highlighted the challenges towards clinical translation. This work demonstrated the

viability of combining multiple sub-cultured primary human cell types in a single relatively soft biomaterial, sharing one culture medium. Multi-cell-differentiation into all relevant lineages was successful in gelatine-based hydrogels, cultured in a tailored endothelial-osteogenic combination medium. Moreover, the presented results were reproducible for MSCs and ECFCs isolated from various donors and applied in different combinations in the co-cultures, further underlining the attainability of a clinical translation.

Conclusions

A complex human tissue model was created with an endothelium-covered central channel, surrounded by stabilised capillary-like structures and osteogenic cells. The simultaneous differentiation of multiple cell types required a tailored medium, which was found in a combination of ODM and EGM-2, inducing the desired early differentiations for this tissue model. Furthermore, combining multiple clinically-relevant human primary cells in one tissue-engineered construct resulted in a viable approach. Therefore, the present work showed the feasibility of engineering complex tissue constructs, paving the way for scale-up approaches with the potential to finally overcome the challenge of vascularisation of engineered tissues.

Acknowledgements

The authors are grateful to Joao Garcia, who designed the mould to fabricate the channelled silicone moulds that were printed by Cetma (Brindisi, Italy), and Alessia Longoni for helping with the FACS analysis. Further acknowledgement goes to Chris van Dijk from Dr Caroline Cheng's group for his help in the transduction of ECFCs with GFP and Mattie van Rijen for his contributions to the histology. This research was partially funded by the European Union FP7-MC-IRSES 'SkelGEN' project under grant agreement Nr. 318553.

References

Au P, Tam J, Fukumura D, Jain RK (2008) Bone marrow-derived mesenchymal stem cells facilitate engineering of long-lasting functional vasculature. Blood **111**: 4551-4558.

Baldwin J, Antille M, Bonda U, De-Juan-Pardo EM, Khosrotehrani K, Ivanovski S, Petcu EB, Hutmacher DW (2014) *In vitro* pre-vascularisation of tissue-engineered constructs: a co-culture perspective. Vasc Cell **6**: 13.

Bersini S, Gilardi M, Arrigoni C, Talo G, Zamai M, Zagra L, Caiolfa V, Moretti M (2016) Human *in vitro* 3D co-culture model to engineer vascularized bone-mimicking tissues combining computational tools and statistical experimental approach. Biomaterials **76**: 157-172.

Bertassoni LE, Cecconi M, Manoharan V, Nikkhah M, Hjortnaes J, Cristino AL, Barabaschi G, Demarchi D, Dokmeci MR, Yang Y, Khademhosseini A (2014) Hydrogel bioprinted microchannel networks for vascularization of tissue engineering constructs. Lab Chip **14**: 2202-2211.

Blache U, Metzger S, Vallmajo-Martin Q, Martin I, Djonov V, Ehrbar M (2016) Dual role of mesenchymal stem cells allows for microvascularized bone tissue-like environments in PEG hydrogels. Adv Healthc Mater **5**: 489-498.

Boere KWM, Visser J, Seyednejad H, Rahimian S, Gawlitta D, van Steenbergen MJ, Dhert WJA, Hennink WE, Vermonden T, Malda J (2014) Covalent attachment of a three-dimensionally printed thermoplast to a gelatin hydrogel for mechanically enhanced cartilage constructs. Acta Biomater **10**: 2602-2611.

Bolander ME, Robey PG, Fisher LW, Conn KM, Prabhakar BS, Termine JD (1989) Monoclonal-antibodies against osteonectin show conservation of epitopes across species. Calcif Tissue Int **45**: 74-80.

Butt OI, Carruth R, Kutala VK, Kuppusamy P, Moldovan NI (2007) Stimulation of peri-implant vascularization with bone marrow-derived progenitor cells: monitoring by *in vivo* EPR oximetry. Tissue Eng **13**: 2053-2061.

Byambaa B, Annabi N, Yue K, Trujillo-de Santiago G, Alvarez MM, Jia W, Kazemzadeh-Narbat M, Shin SR, Tamayol A, Khademhosseini A (2017) Bioprinted osteogenic and vasculogenic patterns for engineering 3D bone tissue. Adv Healthc Mater **16**. DOI: 10.1002/adhm.201700015.

Carmeliet P, Jain RK (2000) Angiogenesis in cancer and other diseases. Nature **407**: 249-257.

Castano-Izquierdo H, Alvarez-Barreto J, van den Dolder J, Jansen JA, Mikos AG, Sikavitsas VI (2007) Pre-culture period of mesenchymal stem cells in osteogenic media influences their *in vivo* bone forming potential. J Biomed Mater Res A **82**: 129-138.

Celikkin N, Mastrogiacomo S, Jaroszewicz J, Walboomers XF, Swieszkowski W (2018) Gelatin methacrylate scaffold for bone tissue engineering: the influence of polymer concentration. J Biomed Mater Res A **106**: 201-209.

Chen YC, Lin RZ, Qi H, Yang Y, Bae H, Melero-Martin JM, Khademhosseini A (2012) Functional human vascular network generated in photocrosslinkable gelatin methacrylate hydrogels. Adv Funct Mater **22**: 2027-2039.

de Souza LEB, Malta TM, Haddad SK, Covas DT (2016) Mesenchymal stem cells and pericytes: to what extent are they related?. Stem Cells Dev **25**: 1843-1852.

Ehrbar M, Sala A, Lienemann P, Ranga A, Mosiewicz K, Bittermann A, Rizzi SC, Weber FE, Lutolf MP (2011) Elucidating the role of matrix stiffness in 3D cell migration and remodeling. Biophys J **100**: 284-293.

Gawlitta D, Fledderus JO, van Rijen MH, Dokter I, Alblas J, Verhaar MC, Dhert WJ (2012) Hypoxia impedes vasculogenesis of *in vitro* engineered bone. Tissue Eng Part A **18**: 208-218.

Gimbrone MA, Jr., Cotran RS, Folkman J (1974) Human vascular endothelial cells in culture. Growth and DNA synthesis. J Cell Biol **60**: 673-684.

Gotman I, Ben-David D, Unger RE, Bose T, Gutmanas EY, Kirkpatrick CJ (2013) Mesenchymal stem cell proliferation and differentiation on load-bearing trabecular Nitinol scaffolds. Acta Biomater **9**: 8440-8448.

Gruber R, Kandler B, Holzmann P, Vögele-Kadletz M, Losert U, Fischer MB, Watzek G (2005) Bone marrow stromal cells can provide a local environment that favors migration and formation of tubular structures of endothelial cells. Tissue Eng **11**: 896-903.

Hasan A, Paul A, Memic A, Khademhosseini A (2015) A multilayered microfluidic blood vessel-like structure. Biomed Microdevices **17**: 88.

Huebsch N, Arany PR, Mao AS, Shvartsman D, Ali OA, Bencherif SA, Rivera-Feliciano J, Mooney DJ (2010) Harnessing traction-mediated manipulation of the cell/matrix interface to control stem-cell fate. Nature Materials **9**: 518-526.

Hung SC, Pochampally RR, Chen SC, Hsu SC, Prockop DJ (2007) Angiogenic effects of human multipotent stromal cell conditioned medium activate the PI3K-Akt pathway in hypoxic endothelial cells to inhibit apoptosis, increase survival, and stimulate angiogenesis. Stem Cells **25**: 2363-2370.

Jin GZ, Han CM, Kim HW (2015) *In vitro* co-culture strategies to prevascularization for bone regeneration: a brief update. Tissue Eng Regen Med **12**: 69-79.

Kanczler JM, Oreffo ROC (2008) Osteogenesis and angiogenesis: the potential for engineering bone. Eur Cell Mater **15**: 100-114.

Kazemzadeh-Narbat M, Rouwkema J, Annabi N, Cheng H, Ghaderi M, Cha BH, Aparnathi M, Khalilpour A, Byambaa B, Jabbari E, Tamayol A, Khademhosseini A (2017) Engineering photocrosslinkable bicomponent hydrogel constructs for creating 3D vascularized bone. Adv Healthc Mater **6**. DOI: 10.1002/adhm.201601122.

Klotz BJ, Gawlitta D, Rosenberg AJWP, Malda J, Melchels FPW (2016) Gelatin-methacryloyl hydrogels: towards biofabrication-based tissue repair. Trends Biotechnol **34**: 394-407.

Kolbe M, Xiang Z, Dohle E, Tonak M, Kirkpatrick CJ, Fuchs S (2011) Paracrine effects influenced by cell culture medium and consequences on microvessel-like structures in cocultures of mesenchymal stem cells and outgrowth endothelial cells. Tissue Eng Part A **17**: 2199-2212.

Kolesky DB, Homan KA, Skylar-Scott MA, Lewis JA (2016) Three-dimensional bioprinting of thick vascularized tissues. Proc Natl Acad Sci U S A **113**: 3179-3184.

Kolesky DB, Truby RL, Gladman AS, Busbee TA, Homan KA, Lewis JA (2014) 3D bioprinting of vascularized, heterogeneous cell-laden tissue constructs. Adv Mater **26**: 3124-3130.

Koshy ST, Ferrante TC, Lewin SA, Mooney DJ (2014) Injectable, porous, and cell-responsive gelatin cryogels. Biomaterials **35**: 2477-2487.

Lafage-Proust MH, Roche B, Langer M, Cleret D, Vanden Bossche A, Olivier T, Vico L (2015) Assessment of bone vascularization and its role in bone remodeling. Bonekey Rep **4**: 662.

Langer RS, Vacanti JP (1999) Tissue engineering: the challenges ahead. Sci Am **280**: 86-89.

Lee JH, Kim SW, Kim UK, Oh SH, June-Kim S, Park BW, Kim JH, Hah YS, Kim DR, Rho GJ, Maeng GH, Jeon RH, Lee HC, Kim JR, Kim GC, Byun JH (2013) Generation of osteogenic construct using periosteal-derived osteoblasts and polydioxanone/pluronic F127 scaffold with periosteal-derived CD146 positive endothelial-like cells. J Biomed Mater Res A **101**: 942-953.

Lee VK, Lanzi AM, Ngo H, Yoo SS, Vincent PA, Dai GH (2014) Generation of multi-scale vascular network system within 3D hydrogel using 3D bio-printing technology. Cell Mol Bioeng **7**: 460-472.

Levenberg S, Rouwkema J, Macdonald M, Garfein ES, Kohane DS, Darland DC, Marini R, van Blitterswijk CA, Mulligan RC, D'Amore PA, Langer R (2005) Engineering vascularized skeletal muscle tissue. Nat Biotechnol **23**: 879-884.

Lim KS, Alves MH, Poole-Warren LA, Martens PJ (2013) Covalent incorporation of non-chemically modified gelatin into degradable PVA-tyramine hydrogels. Biomaterials **34**: 7097-7105.

Lim KS, Kundu J, Reeves A, Poole-Warren LA, Kundu SC, Martens PJ (2012) The influence of silkworm species on cellular interactions with novel PVA/silk sericin hydrogels. Macromol Biosci **12**: 322-332.

Loessner D, Meinert C, Kaemmerer E, Martine LC, Yue K, Levett PA, Klein TJ, Melchels FPW, Khademhosseini A, Hutmacher DW (2016) Functionalization, preparation and use of cell-laden gelatin methacryloyl-based hydrogels as modular tissue culture platforms. Nature Protocols **11**: 727-746.

Ma J, van den Beucken JJ, Yang F, Both SK, Cui FZ, Pan J, Jansen JA (2011) Coculture of osteoblasts and endothelial cells: optimization of culture medium and cell ratio. Tissue Eng Part C Methods **17**: 349-357.

Mekhileri NV, Lim KS, Brown GCJ, Mutreja I, Schon BS, Hooper GJ, Woodfield TBF (2018) Automated 3D bioassembly of micro-tissues for biofabrication of hybrid tissue engineered constructs. Biofabrication **10**: 024103.

Miller JS, Stevens KR, Yang MT, Baker BM, Nguyen DH, Cohen DM, Toro E, Chen AA, Galie PA, Yu X, Chaturvedi R, Bhatia SN, Chen CS (2012) Rapid casting of patterned vascular networks for perfusable engineered three-dimensional tissues. Nat Mater **11**: 768-774.

Nguyen AH, McKinney J, Miller T, Bongiorno T, McDevitt TC (2015) Gelatin methacrylate

microspheres for controlled growth factor release. Acta Biomater **13**: 101-110.

Nandi S, Winter HH (2005) Swelling behavior of partially cross-linked polymers: a ternary system. Macromolecules **38**: 4447-4455.

Nichol JW, Koshy ST, Bae H, Hwang CM, Yamanlar S, Khademhosseini A (2010) Cell-laden microengineered gelatin methacrylate hydrogels. Biomaterials **31**: 5536-5544.

Niemisto A, Dunmire V, Yli-Harja O, Zhang W, Shmulevich I (2005) Robust quantification of *in vitro* angiogenesis through image analysis. IEEE Transactions on Medical Imaging **24**: 549-553.

Nilasaroya A, Poole-Warren LA, Whitelock JM, Martens PJ (2008) Structural and functional characterisation of poly(vinyl alcohol) and heparin hydrogels. Biomaterials **29**: 4658-4664.

Occhetta P, Visone R, Russo L, Cipolla L, Moretti M, Rasponi M (2015) VA-086 methacrylate gelatine photopolymerizable hydrogels: a parametric study for highly biocompatible 3D cell embedding. J Biomed Mater Res A **103**: 2109-2117.

Rouwkema J, Khademhosseini A (2016) Vascularization and angiogenesis in tissue engineering: beyond creating static networks. Trends Biotechnol **34**: 733-745.

Schuurman W, Khristov V, Pot MW, van Weeren PR, Dhert WJ, Malda J (2011) Bioprinting of hybrid tissue constructs with tailorable mechanical properties. Biofabrication **3**: 021001.

Tan S, Fang JY, Yang Z, Nimni ME, Han B (2014) The synergetic effect of hydrogel stiffness and growth factor on osteogenic differentiation. Biomaterials **35**: 5294-5306.

Unger RE, Dohle E, Kirkpatrick CJ (2015) Improving vascularization of engineered bone through the generation of pro-angiogenic effects in co-culture systems. Adv Drug Deliv Rev **94**: 116-125.

Urbaczek AC, Leao P, Souza FZR, Afonso A, Vieira Alberice J, Cappelini LTD, Carlos I Z, Carrilho E (2017) Endothelial cell culture under perfusion on a polyester-toner microfluidic device. Sci Rep **7**: 10466.

Van den Bulcke AI, Bogdanov B, De Rooze N, Schacht EH, Cornelissen M, Berghmans H (2000) Structural and rheological properties of methacrylamide modified gelatin hydrogels. Biomacromolecules **1**: 31-38.

Visser J, Melchels FPW, Jeon JE, van Bussel EM, Kimpton LS, Byrne HM, Dhert WJA, Dalton PD, Hutmacher DW, Malda J (2015) Reinforcement of hydrogels using three-dimensionally printed microfibres. Nat Commun **6**: 6933.

Wen JH, Vincent LG, Fuhrmann A, Choi YS, Hribar KC, Taylor-Weiner H, Chen S, Engler AJ (2014) Interplay of matrix stiffness and protein tethering in stem cell differentiation. Nat Mater **13**: 979-987.

Zheng Y, Chen J, Lopez JA (2015) Flow-driven assembly of VWF fibres and webs in *in vitro* microvessels. Nat Commun **6**: 7858.

Zhu W, Qu X, Zhu J, Ma X, Patel S, Liu J, Wang P, Lai CS, Gou M, Xu Y, Zhang K, Chen S (2017) Direct 3D bioprinting of prevascularized tissue constructs with complex microarchitecture. Biomaterials **124**: 106-115.

Discussion with Reviewer

Bara Jennifer: Do the authors know if the formation of vessel-like structures was dependent upon cell migration and assembly or rather proliferation of the ECFCs?

Authors: Angiogenesis is a complex multistep process involving both migration and proliferation of endothelial cells (DeCicco-Skinner *et al.*, 2014, additional reference; Northon and Popel, 2016, additional reference). However, the question as to whether vessel formation was dependent on cell migration or proliferation was not evaluated. As a co-culture model comprising MSCs and ECFCs was employed, it was difficult to track the migration and proliferation of both cells. However, gelMA hydrogels of higher DoF resulted in constructs of higher compressive modulus, which impeded cellular spreading and formation of vessel-like structures.

Additional References

DeCicco-Skinner KL, Henry GH, Cataisson C, Tabib T, Gwilliam JC, Watson NJ, Bullwinkle EM, Falkenburg L, O'Neill RC, Morin A, Wiest JS (2014) Endothelial cell rube formation assay for the *in vitro* study of angiogenesis. J Vis Exp **91**: e51312.

Norton K, Popel AS (2016) Effects of endothelial cell proliferation and migration rates in a computational model of sprouting angiogenesis. Scientific Reports **6**: 36992.

Editor's note: The Scientific Editor responsible for this paper was Stephen Ferguson.